

## Two Polymeric Compounds Built from Mononuclear and Tetrameric Squarate–Copper(II) Complexes by Deprotonation of 3,3-Bis(2-imidazolyl)propionic Acid (HBIP). Synthesis, Crystal Structure, and Magnetic Characterization of $[\text{Cu}(\text{HBIP})(\text{BIP})](\text{C}_4\text{O}_4)_{1/2} \cdot 2\text{H}_2\text{O}$ and $[\{\text{Cu}(\text{BIP})(\text{OH}_2)\}_4(\mu\text{-C}_4\text{O}_4)](\text{ClO}_4)_2 \cdot 4\text{H}_2\text{O}$

Y. Akhriff, J. Server-Carrió, A. Sancho, J. García-Lozano, E. Escrivá, and L. Soto\*

Departament de Química Inorgànica, Universitat de València, c/Vicent Andrés Estellés, s/n, 46100 Burjassot, València, Spain

Received June 20, 2001

Two polynuclear copper(II)–squarate compounds of formulas  $[\text{Cu}(\text{HBIP})(\text{BIP})](\text{C}_4\text{O}_4)_{1/2} \cdot 2\text{H}_2\text{O}$  (**1**) and  $[\{\text{Cu}(\text{BIP})(\text{OH}_2)\}_4(\mu\text{-C}_4\text{O}_4)](\text{ClO}_4)_2 \cdot 4\text{H}_2\text{O}$  (**2**) (HBIP = 3,3-bis(2-imidazolyl)propionic acid) have been synthesized and characterized by single-crystal X-ray diffraction. Both compounds crystallize in the triclinic system, space group  $P\bar{1}$ , with  $a = 7.947(1)$  Å,  $b = 12.327(4)$  Å,  $c = 13.150(3)$  Å,  $\alpha = 113.91(2)^\circ$ ,  $\beta = 99.85(2)^\circ$ ,  $\gamma = 90.02(2)^\circ$  for compound **1** and  $a = 8.010(1)$  Å,  $b = 13.073(1)$  Å,  $c = 14.561(1)$  Å,  $\alpha = 72.13(1)^\circ$ ,  $\beta = 80.14(1)^\circ$ ,  $\gamma = 84.02(1)^\circ$  for compound **2**. The structure of compound **1** can be viewed as made up of  $[\text{Cu}(\text{HBIP})(\text{BIP})]$  units linked together by the BIP carboxylate groups to form a one-dimensional chain structure along the  $a$  axis in the crystal. The copper ion is five-coordinated (CuN<sub>4</sub>O chromophore) with BIP and HBIP acting as tridentate and bidentate ligands, respectively. The coordination geometry is intermediate between SP and TBP. The structure of compound **2** is made of infinite chains built from cationic tetranuclear  $[\{\text{Cu}(\text{BIP})(\text{OH}_2)\}_4(\mu\text{-C}_4\text{O}_4)]^{2+}$  complex units, two uncoordinated perchlorate anions, and four water molecules of crystallization. The squarate group bridges the copper(II) ions, while BIP acts as a tridentate ligand, connecting through its carboxylate group the tetrameric units along the  $a$  axis. The two crystallographically independent copper(II) ions are pentacoordinated within a distorted square-based pyramid. Electronic and EPR spectra are consistent with the crystallographic data. Both compounds follow a Curie–Weiss law with very low values of  $\theta$  ( $-0.13$  and  $+0.12$  K). In compound **2**, the weak ferromagnetism interaction is discussed on the basis of the structural features and correlated with published magnetostructural data on similar squarate-bridged copper(II) compounds.

### Introduction

During the past few years there has been a growing interest in the design of coordination polymers containing bridging ligands between metal centers to form one-, two-, and three-dimensionally connected polymer networks. One of the main interests of this field is based on the need for the design and synthesis of novel functional materials with highly ordered structures containing paramagnetic metal centers to provide molecular-based magnets.<sup>1</sup> These systems are also of interest owing to their potential applications as model compounds that would mimic binuclear rearrangements occurring in metalloenzymes.<sup>2</sup> This is especially relevant when imidazole and carboxylate moieties are used as ligands, since they are ubiquitous in biomolecules such as proteins and nucleic acids.<sup>3</sup>

The structural topology of coordination polymers can be specifically designed by selection of such parameters as the stereoelectronic preferences of the metal ion, spatial disposition of binding sites on the ligands, and reaction conditions, to yield a desired architecture. In addition to the strong chemical bonds, the presence of weak interactions such as directional hydrogen bonds and  $\pi$ – $\pi$  stacking interactions may turn out to play a decisive role in determining the resulting architecture.<sup>4</sup> In this context, the protonated and deprotonated forms of 3,3-bis(2-imidazolyl)propionic acid (HBIP)<sup>5</sup>—an imidazole–carboxylate polyfunctional ligand—has proved to be useful ligands in the synthesis of systems showing variable nuclearity. HBIP, which

can act as a bidentate chelating ligand, has also the capacity of functioning, via deprotonation of the carboxylate group, as a

- (1) (a) Kahn, O. *Angew. Chem., Int. Ed. Engl.* **1985**, *24*, 834. (b) Kahn, O. *Molecular Magnetism*; VCH: Weinheim, Germany, 1993. (c) *Magnetism: A Supramolecular Function*; Kahn, O., Ed.; NATO ASI Series C484; Kluwer Academic Publishers: Dordrecht, The Netherlands, 1996. (d) *Molecular Magnetism: From the Molecular Assemblies to the Devices*; Coronado, E., Delhaes, P., Gatteschi, D., Miller, J. S., Eds.; NATO ASI Series E321; Kluwer Academic Publishers: Dordrecht, The Netherlands, 1996. (e) Decurtins, S.; Schmalte, H. W.; Pellaux, R.; Schnewly, P.; Hauser, A. *Inorg. Chem.* **1996**, *35*, 1451. (f) Román, P.; Guzmán-Miralles, C.; Luque, A.; Beitia, J. I.; Cano, J.; Lloret, F.; Julve, M.; Alvarez, S. *Inorg. Chem.* **1996**, *35*, 3741. (g) Decurtins, S.; Schmalte, H. W.; Pellaux, R.; Fischer, P.; Hauser, A. *Mol. Cryst. Liq. Cryst.* **1997**, *305*, 227. (h) Pellaux, R.; Schmalte, H. W.; Huber, R.; Fischer, P.; Hauss, T.; Ouladdiaf, B.; Decurtins, S. *Inorg. Chem.* **1997**, *36*, 2301. (i) Vicente, R.; Escuer, A.; Ferretjans, J.; Stoeckli-Evans, H.; Solans, X.; Font-Bardia, M. *J. Chem. Soc., Dalton Trans.* **1997**, 167. (j) Cano, J.; Alemany, P.; Alvarez, S.; Verdager, M.; Ruiz, E. *Chem. Eur. J.* **1998**, *4*, 476. (k) Castillo, O.; Muga, I.; Luque, A.; Gutiérrez-Zorrilla, J. M.; Sertucha, J.; Vitoria, P.; Román, P. *Polyhedron* **1999**, *18*, 1235. (l) Castillo, O.; Luque, A.; Sertucha, J.; Román, P.; Lloret, F. *Inorg. Chem.* **2000**, *39*, 6142.
- (2) (a) *Bioinorganic Chemistry*; Bertini, I., Gray, H. B., Lippard, S. J., Valentine, J. S., Eds.; University Science Books: Mill Valley, CA, 1994. (b) Solomon, E. I.; Lowery, M. D.; Root, D. E.; Hemming, B. L. *Mechanistic Bioinorganic Chemistry*; American Chemical Society: Washington, DC, 1995. (c) Solomon, E. I.; Sundaram, U. M.; Machonkin, T. E. *Chem. Rev.* **1996**, *96*, 2563. (d) Holm, R. H.; Kennepohl, P.; Solomon, E. I. *Chem. Rev.* **1996**, *96*, 2239. (e) Tabbi, G.; Driessen, W. L.; Reedijk, J.; Bonomo, R. P.; Veldman, N.; Spek, A. L. *Inorg. Chem.* **1997**, *36*, 1168.

dinucleating bridging ligand. In addition to metal binding sites, this ligand also contains hydrogen-bonding functionalities that are retained upon complexation. Recently, the HBIP ligand has allowed the construction of different transition metal networks ranging from mononuclear entities such as  $[\text{Cu}(\text{HBIP})(\text{BIP})-(\text{ONO}_2)]_n^6$  and  $[\text{Cu}(\text{HBIP})(\text{C}_2\text{O}_4)(\text{OH}_2)]_2 \cdot 2\text{H}_2\text{O}^7$  through dimeric compounds, such as  $[\{\text{Cu}(\text{HBIP})\text{Cl}\}_2(\mu\text{-C}_2\text{O}_4)]_2 \cdot 2\text{H}_2\text{O}^7$  to polymeric ones such as  $[\{\text{Cu}(\text{BIP})\}_2(\mu\text{-C}_2\text{O}_4)]_n \cdot 6\text{H}_2\text{O}^7$ . This latter structure consists of infinite ladder-like chain motifs. In all these cases, monomers as well as chains interact together to give sheets, which in turn interact to give three-dimensional networks. These chains and three-dimensional networks result from weak H-bond interactions involving NH, N, COOH, and  $\text{COO}^-$  moieties of the HBIP and other free as well as coordinated exogenous ligands. These molecules generally undergo magnetic exchange interactions, where the magnitude of the exchange coupling depends on the dimensional arrangement of the molecules in the lattice. Interconversion between monomers and polymers is achieved by controlling experimental conditions such as pH of crystallization, molar ratios, and charge neutralization. Following our research on bridged systems of variable nuclearity, we herein report the synthesis and structural, spectroscopic, and magnetic characterization of two HBIP-containing copper(II) squarate derivatives in which HBIP and squarate ligands show different coordinating behavior. The two stoichiometrically related complexes,  $[\text{Cu}(\text{HBIP})(\text{BIP})-(\text{C}_4\text{O}_4)_{1/2} \cdot 2\text{H}_2\text{O}$  (**1**) and  $[\{\text{Cu}(\text{BIP})(\text{OH}_2)\}_4(\mu\text{-C}_4\text{O}_4)](\text{ClO}_4)_2 \cdot 4\text{H}_2\text{O}$  (**2**), are obtained by using different Cu:HBIP molar ratios. Compound **1** exhibits an extended monodimensional array built of chains interconnected by the carboxylate moiety of BIP, with the squarate group acting as the counterion. Compound **2** is the first tetranuclear copper(II)–BIP family complex in which a weak ferromagnetic coupling takes place through the squarate ion acting in a  $\mu\text{-1,2,3,4}$  coordination mode. Magnetic and EPR results are discussed with respect to the crystal structures of **1** and **2** and compared with analogous  $\mu$ -squarate complexes previously reported.

## Experimental Section

**Materials.** CAUTION! Perchlorate salts of metal complexes with organic ligands are potentially explosive. Only a small amount of material should be prepared, and it should be handled with caution. 3,3-Bis(2-imidazolyl)propionic acid (HBIP) was prepared according to Joseph et al.<sup>8</sup> and characterized by  $^1\text{H}$  NMR,  $^{13}\text{C}$  NMR, and IR spectroscopy and powder X-ray diffraction. All other reagents were used as supplied. Elemental analyses (C, H, N, Cl) were performed by Servei de Microanàlisi, Consell Superior d'Investigacions Científiques, Barcelona, Spain.

- (3) (a) Várnagy, K.; Sóvágó, I.; Ágoston, K.; Likó, Z.; Süli-Vargha, H.; Sanna, D.; Micera, G. *J. Chem. Soc., Dalton Trans.* **1994**, 2939. (b) Dominguez-Vera, J. M.; Galvez, N.; Colacio, E.; Cuesta, R.; Costes, J.-P.; Laurent, J.-P. *J. Chem. Soc., Dalton Trans.* **1996**, 861. (c) Bhalla, R.; Helliwell, M.; Garner, C. D. *Inorg. Chem.* **1997**, *36*, 2944. (d) Kodera, M.; Terasako, N.; Kita, T.; Tachi, Y.; Kano, K.; Yamazaki, M.; Koikawa, M.; Tokii, T. *Inorg. Chem.* **1997**, *36*, 3861. (e) Place, C.; Zimmermann, J. L.; Mulliez, E.; Guillot, G.; Bois, C.; Chottard, J. C. *Inorg. Chem.* **1998**, *37*, 4030.
- (4) (a) Karle, I. L.; Ranganathan, D.; Haridas, V. *J. Am. Chem. Soc.* **1996**, *118*, 7128. (b) Alleyne, B. D.; Hall, L. A.; Hosein, H.-A.; Jaggernauth, H.; White, A. J. P.; Williams, D. J. *J. Chem. Soc., Dalton Trans.* **1998**, 3845. (c) Lopez, S.; Keller, S. W. *Inorg. Chem.* **1999**, *38*, 1883.
- (5) (a) Gimeno, B.; Soto, L.; Sancho, A.; Dahan, F.; Legros, J. P. *Acta Crystallogr.* **1992**, *C48*, 1671. (b) Gimeno, B.; Sancho, A.; Soto, L.; Legros, J. P. *Acta Crystallogr.* **1996**, *C52*, 1226.
- (6) Sancho, A.; Gimeno, B.; Amigó, J. M.; Ochando, L. E.; Debaerdaemaeker, T.; Folgado, J. V.; Soto, L. *Inorg. Chim. Acta* **1996**, *248*, 153.
- (7) Akhriff, Y.; Server-Carrió, J.; Sancho, A.; García-Lozano J.; Escrivá, E.; Folgado, J. V.; Soto, L. *Inorg. Chem.* **1999**, *38*, 1174.
- (8) Joseph, M.; Leigt, T.; Swain, M. L. *Synthesis* **1977**, 459.

**[Cu(HBIP)(BIP)](C<sub>4</sub>O<sub>4</sub>)<sub>1/2</sub>·2H<sub>2</sub>O (**1**).** Aqueous solutions of HBIP (0.25 mmol, 30 mL) and H<sub>2</sub>C<sub>4</sub>O<sub>4</sub> (0.062 mmol, 1.25 mL) were mixed together. Addition of the resulting solution to an aqueous solution of CuCl<sub>2</sub>·2H<sub>2</sub>O (0.125 mmol, 1.25 mL) yielded a green solution, which was allowed to stand at room temperature for about 1 day to produce the complex **1** as blue crystals. The resulting crystals were separated by filtration, washed with water, and ethanol, and dried to constant weight at 60 °C. Anal. Calcd for C<sub>20</sub>H<sub>23</sub>N<sub>8</sub>O<sub>8</sub>Cu (**1**): C, 42.37; H, 4.10; N, 19.77; Cu, 11.21. Found: C, 41.96; H, 3.98; N, 19.60; Cu, 11.38.

**[[Cu(BIP)(OH<sub>2</sub>)]<sub>4</sub>(μ-C<sub>4</sub>O<sub>4</sub>)](ClO<sub>4</sub>)<sub>2</sub>·4H<sub>2</sub>O (**2**).** Aqueous solutions of HBIP (0.25 mmol, 25 mL), H<sub>2</sub>C<sub>4</sub>O<sub>4</sub> (0.125 mmol, 1.25 mL), NaClO<sub>4</sub> (0.5 mmol, 5 mL), and CuCl<sub>2</sub>·2H<sub>2</sub>O (0.25 mmol, 2.5 mL) were mixed together. The resulting solution was allowed to stand at room temperature for about 2 days to produce single blue crystals of complex **2**. The resulting crystals were separated by filtration and washed with water and ethanol. Anal. Calcd for C<sub>40</sub>H<sub>52</sub>N<sub>16</sub>O<sub>28</sub>Cl<sub>2</sub>Cu<sub>4</sub> (**2**): C, 31.40; H, 3.43; N, 14.65; Cl, 4.62; Cu, 16.62. Found: C, 31.60; H, 3.28; N, 14.50; Cl, 4.50; Cu, 16.78.

**X-ray Crystallographic Studies of 1 and 2.** The selected prismatic crystals of the complexes were mounted on an Enraf-Nonius CAD4 single-crystal diffractometer, and intensity measurements were carried out at room temperature using graphite-monochromated Mo K $\alpha$  radiation ( $\lambda = 0.71070$  Å). The unit cell dimensions were determined from the angular settings of 25 reflections. The intensity data were measured between the limits  $1^\circ < \theta < 25^\circ$  using the  $\omega/2\theta$  scan technique. Data reduction was performed with the X-RAY76 system.<sup>9</sup> Empirical absorption corrections were applied following the procedure DIFABS.<sup>10</sup>

The structures were solved by direct methods using the program SIR92.<sup>11</sup> Non-hydrogen atoms were anisotropically refined by least-squares on  $F^2$  with SHELXL97.<sup>12</sup> Hydrogens bonded to C atoms were placed at calculated positions, and hydrogens bonded to O and N atoms were located by difference synthesis. All of them were kept fixed in the refinement with isotropic temperature factors related to their bonded atom. Atomic scattering factors and anomalous dispersion corrections were taken from ref 13. Geometrical calculations were made with PARTS.<sup>14</sup> Graphical representations were produced with ORTEP3 for Windows.<sup>15</sup>

**Complex 1.** A suitable blue crystal (approximate dimensions  $0.15 \times 0.15 \times 0.30$  mm<sup>3</sup>) was selected. The unit cell dimensions were determined in the range  $8^\circ < \theta < 15^\circ$ ; 4540 reflections were measured in the  $hkl$  ranges 0 to 9,  $-14$  to 14, and  $-15$  to 15. From the 4085 independent reflections 2409 were considered observed with  $I > 2\sigma(I)$ . Minimum and maximum absorption correction coefficients were 0.729 and 0.912, respectively. There were 334 refined parameters. After the final refinement: goodness of fit on  $F^2 = 0.971$  and largest difference peak and hole = 0.35 and  $-0.45$  e Å<sup>-3</sup>, respectively.

**Complex 2.** A suitable blue crystal with approximate size  $0.20 \times 0.20 \times 0.25$  mm<sup>3</sup> was selected. The unit cell dimensions were determined in the range  $10^\circ < \theta < 17^\circ$ ; 5591 reflections were measured in the  $hkl$  ranges 0 to 9,  $-15$  to 15, and  $-17$  to 17. From the 5029 independent reflections 4177 were considered observed with  $I > 2\sigma(I)$ . Minimum and maximum absorption correction coefficients were 0.648 and 0.760, respectively. There were 406 refined parameters. After the final refinement: goodness of fit on  $F^2 = 1.067$  and largest difference peak and hole = 0.58 and  $-0.56$  e Å<sup>-3</sup>, respectively.

Other relevant data of the crystal structure studies are listed in Table 1. Selected bond distances and angles are listed in Table 2.

- (9) Stewart, J. M.; Machin, P. A.; Dickinson, C. W.; Ammon, H. L.; Heck, H.; Flack, H. *The X-RAY76 System*; Technical Report TR-446; Computer Science Center, University of Maryland: College Park, MD, 1976.
- (10) Walker, N.; Stuart, D. *Acta Crystallogr., Sect. A* **1983**, *39*, 158.
- (11) Altomare, A.; Burla, M. C.; Camalli, M.; Cascarano, G.; Giacovazzo, G.; Guagliardi, A.; Polidori, G. *J. Appl. Crystallogr.* **1994**, *27*, 435.
- (12) Sheldrick, G. M. *SHELXL97*; University of Göttingen: Göttingen, Germany, 1997.
- (13) *International Tables for X-Ray Crystallography*; Kynoch Press: Birmingham, U.K., 1974; Vol. IV, pp 71 and 149.
- (14) Nardelli, M. *Comput. Chem.* **1983**, *7*, 95.
- (15) Farrugia, L. J. *J. Appl. Crystallogr.* **1997**, *30*, 565.

**Table 1.** Crystallographic Data for [Cu(HBIP)(BIP)](C<sub>4</sub>O<sub>4</sub>)<sub>1/2</sub>·2H<sub>2</sub>O (**1**) and [Cu(BIP)(OH<sub>2</sub>)<sub>2</sub>]<sub>2</sub>(μ-C<sub>4</sub>O<sub>4</sub>)(ClO<sub>4</sub>)<sub>2</sub>·4H<sub>2</sub>O (**2**)

	<b>1</b>	<b>2</b>
formula	C <sub>20</sub> H <sub>23</sub> N <sub>8</sub> O <sub>8</sub> Cu	C <sub>40</sub> H <sub>52</sub> N <sub>16</sub> O <sub>28</sub> Cl <sub>2</sub> Cu <sub>4</sub>
fw	567.0	1530.0
space group (No.)	P1̄ (2)	P1̄ (2)
a, Å	7.947(1)	8.010(1)
b, Å	12.327(4)	13.073(1)
c, Å	13.150(3)	14.561(1)
α, deg	113.91(2)	72.13(1)
β, deg	99.85(2)	80.14(1)
γ, deg	90.02(2)	84.02(1)
V, Å <sup>3</sup>	1156(1)	1427.6(2)
Z	2	1
λ(Mo Kα), Å	0.71070	0.71070
μ(Mo Kα), cm <sup>-1</sup>	10.01	16.67
ρ(calcd), g cm <sup>-3</sup>	1.63	1.78
T, °C	22	22
R1 <sup>a</sup>	0.060	0.046
wR2 <sup>b</sup>	0.159	0.133

<sup>a</sup> R1 =  $\sum ||F_o| - |F_c|| / \sum |F_o|$  for reflections with  $I > 2\sigma(I)$ . <sup>b</sup> wR2 =  $\{\sum [w(F_o^2 - F_c^2)^2] / \sum [w(F_c^2)^2]\}^{1/2}$  for all reflections;  $w = 1/[\sigma^2(F_o^2) + (aP)^2 + bP]$ , where  $P = [2F_c^2 + F_o^2]/3$  and  $a$  and  $b$  are constants set by the program.

**Physical Measurements.** IR spectra (KBr pellets) were recorded on a Pye Unicam SP 2000 spectrophotometer in the 4000–200 cm<sup>-1</sup> region. Diffuse reflectance spectra were obtained using a Perkin-Elmer Lambda 9 UV/vis/IR spectrophotometer. Polycrystalline powder EPR spectra were recorded at room temperature on a Bruker ESP-300 equipped with a variable temperature device. Magnetic susceptibility was measured by means of a commercial SQUID magnetometer, Quantum Design model MPMS7 down to 1.8 K.

## Results and Discussion

Reactions between copper(II) ions, HBIP ligand, and squarate anion yield complexes **1** and **2**, which undergo interconversion reactions affording alternative synthetic procedures. Key steps of the synthetic sequences are shown in Scheme 1. It should be pointed out that complex **1** contains both HBIP and BIP ligands with carboxylate groups protonated and deprotonated, respectively.

**Crystal Structure of 1.** The structure of the complex can be viewed as made up of [Cu(HBIP)(BIP)] units, uncoordinated squarate anions, and lattice water molecules. Figure 1 shows a perspective view of the asymmetric unit and the atomic-numbering scheme. Interatomic bond distances and angles are given in Table 2. These [Cu(HBIP)(BIP)] units are linked together by the BIP carboxylate groups to form a one-dimensional chain structure along the  $a$  axis in the crystal. The separation between two neighboring copper atoms along the chain atoms is 7.947(1) Å. Adjacent chains interact through van der Waals contacts and hydrogen bonds between squarate and carboxylic groups, nitrogen atoms of the imidazole moieties, and water molecules to give the three-dimensional network.

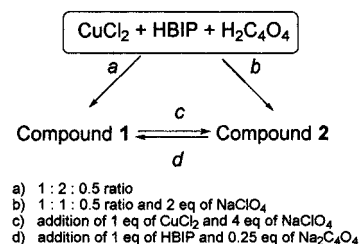
The copper ion is five-coordinated (CuN<sub>4</sub>O chromophore) with BIP and HBIP acting as tridentate and bidentate ligands, respectively. The coordination geometry is intermediate between SP and TBP. Considering the complex as SP, then one imidazole nitrogen atom N(23) of the HBIP occupies the axial position. Basal coordination positions are occupied by the other imidazole nitrogen atoms N(22), N(12), N(13) and an oxygen O(11)<sup>i</sup> from the BIP carboxylate group of an adjacent [Cu(HBIP)(BIP)] unit. The Cu–N distances in the basal plane range from 1.986(5) to 2.017(5) Å, shorter than the apical Cu–N(23) distance (2.140(5) Å). The Cu–O(11)<sup>i</sup> bond length (2.041(4) Å) is longer than the Cu–O(equatorial) reported for [Cu(BIP)]<sub>2</sub>(μ-C<sub>2</sub>O<sub>4</sub>)·6H<sub>2</sub>O<sup>7</sup>

**Table 2.** Selected Bond Lengths (Å) and Angles (deg) for Complexes **1** and **2**<sup>a</sup>

Copper(II) Coordination Sphere			
<b>Complex 1</b>			
Cu–N(12)	1.989(5)	Cu–N(23)	2.140(5)
Cu–N(13)	2.017(5)	Cu–O(11) <sup>i</sup>	2.041(4)
Cu–N(22)	1.986(5)		
N(12)–Cu–N(13)	89.9(2)	N(13)–Cu–N(23)	104.6(2)
N(12)–Cu–N(22)	175.7(2)	N(13)–Cu–O(11) <sup>i</sup>	150.7(2)
N(12)–Cu–N(23)	93.8(2)	N(22)–Cu–N(23)	88.9(2)
N(12)–Cu–O(11) <sup>i</sup>	88.9(2)	N(22)–Cu–O(11) <sup>i</sup>	87.2(2)
N(13)–Cu–N(22)	92.6(2)	N(23)–Cu–O(11) <sup>i</sup>	104.8(2)
<b>Complex 2</b>			
Cu(1)–N(12)	1.982(3)	Cu(1)–O(3)	2.318(3)
Cu(1)–N(13)	1.978(3)	Cu(1)–O(11) <sup>i</sup>	1.974(3)
Cu(1)–O(13)	2.024(3)		
N(12)–Cu(1)–N(13)	90.4(1)	N(13)–Cu(1)–O(3)	98.5(1)
N(12)–Cu(1)–O(13)	88.7(1)	N(13)–Cu(1)–O(11) <sup>i</sup>	91.3(1)
N(12)–Cu(1)–O(3)	98.6(1)	O(13)–Cu(1)–O(3)	92.7(1)
N(12)–Cu(1)–O(11) <sup>i</sup>	169.8(1)	O(13)–Cu(1)–O(11) <sup>i</sup>	87.8(1)
N(13)–Cu(1)–O(13)	168.8(1)	O(3)–Cu(1)–O(11) <sup>i</sup>	91.2(1)
Cu(2)–N(22)	1.965(3)	Cu(2)–O(4)	2.326(3)
Cu(2)–N(23)	1.973(3)	Cu(2)–O(21) <sup>ii</sup>	1.958(3)
Cu(2)–O(23)	2.007(3)		
N(22)–Cu(2)–N(23)	90.7(1)	N(23)–Cu(2)–O(4)	86.2(1)
N(22)–Cu(2)–O(23)	89.9(1)	N(23)–Cu(2)–O(21) <sup>ii</sup>	91.7(1)
N(22)–Cu(2)–O(4)	101.8(1)	O(23)–Cu(2)–O(4)	92.0(1)
N(22)–Cu(2)–O(21) <sup>ii</sup>	165.2(1)	O(23)–Cu(2)–O(21) <sup>ii</sup>	88.1(1)
N(23)–Cu(2)–O(23)	178.1(1)	O(4)–Cu(2)–O(21) <sup>ii</sup>	92.9(1)
<b>Squarate Anions</b>			
<b>Complex 1</b>			
C(3)–O(3)	1.247(6)	C(3)–C(4)	1.450(6)
C(4)–O(4)	1.240(6)	C(3)–C(4) <sup>iii</sup>	1.444(7)
O(3)–C(3)–C(4)	134.8(5)	O(4)–C(4)–C(3)	136.4(5)
O(3)–C(3)–C(4) <sup>iii</sup>	135.3(5)	O(4)–C(4)–C(3) <sup>iii</sup>	133.3(5)
C(4)–C(3)–C(4) <sup>iii</sup>	89.7(5)	C(3)–C(4)–C(3) <sup>iii</sup>	90.3(5)
<b>Complex 2</b>			
C(3)–O(3)	1.256(5)	C(3)–C(4)	1.458(5)
C(4)–O(4)	1.252(5)	C(3)–C(4) <sup>iii</sup>	1.462(5)
O(3)–C(3)–C(4)	134.6(4)	O(4)–C(4)–C(3)	135.1(4)
O(3)–C(3)–C(4) <sup>iii</sup>	135.6(4)	O(4)–C(4)–C(3) <sup>iii</sup>	134.7(4)
C(4)–C(3)–C(4) <sup>iii</sup>	89.8(3)	C(3)–C(4)–C(3) <sup>iii</sup>	90.2(3)

<sup>a</sup> Symmetry codes: (i)  $x + 1, y, z$ ; (ii)  $x - 1, y, z$ ; (iii)  $-x, -y, -z$ .

## Scheme 1



and also longer than that observed in compound **2** (see below). Deviations from a best least-squares plane through N(13)–N(12)–O(11)<sup>i</sup>–N(22) are –0.258(5), 0.237(5), –0.192(5), and 0.248(5) Å, respectively. The copper atom deviates by 0.290(1) Å toward the axial ligand. The angles around copper atom in the basal plane vary from 87.2(2)° to 92.6(2)°, indicating an appreciable distortion from idealized SP geometry. Such a distortion can be quantitatively characterized using the parameter  $\tau$  as defined by Addison et al.<sup>16</sup> The calculated value  $\tau = 0.40$  (relative to 1 for a regular TBP and 0 for a regular SP) indicates a significant degree of distortion of the coordination polyhedron.

(16) Addison, A. W.; Rao, T. N.; Reedijk, J.; van Rijn, J.; Verschoor, G. *C. J. Chem. Soc., Dalton Trans.* **1984**, 1349.

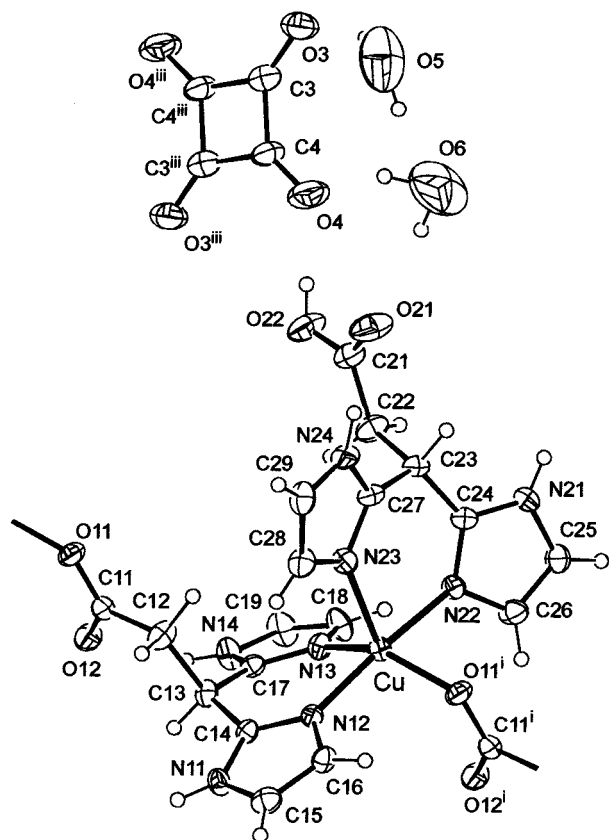


**Figure 1.** ORTEP drawing of the polymeric unit of compound **1** showing the atom-labeling scheme. Thermal ellipsoids are drawn at the 50% probability level. For symmetry codes see Table 2.

Geometries of HBIP and BIP moieties (interatomic distances and angles) are similar to that previously found in HBIP-containing copper(II) compounds.<sup>6,7</sup> The imidazole ring ligands are planar as expected, with deviations from the mean planes not greater than 0.012(7) Å in HBIP and 0.017(6) Å in BIP molecules. The dihedral angles between the two imidazole rings are 27.0(2)° for HBIP and 26.5(2)° for BIP. With regard to the carboxylate group of the BIP ligand, the C–O bond distances satisfy the trend  $C-O_{\text{coord}} > C-O_{\text{uncoord}}$ , as expected from the polarization of the charge density toward the metal-bonded oxygen atoms.

The squarate ion is planar. The whole of its topological parameters (C–C and C–O bond lengths and C–C–C and C–C–O angles, see Table 2) fall in the expected range for a  $C_4O_4$  group with a roughly  $D_{4h}$  symmetry. In order to estimate the delocalization within the squarate groups, Xanthopoulos et al.<sup>17</sup> use the parameters  $\Delta(C-C)$  and  $\Delta(C-O)$  defined as the difference between the shortest and the longest C–C and C–O bonds within the squarate group. A related parameter  $\delta$ , defined as  $\delta = \sum |d(C-C)_i - (d(C-C)_{\text{mean}})| + \sum |d(C-O)_i - (d(C-O)_{\text{mean}})|$  is taken as a good indicator of the asymmetry in the  $C_4O_4$  group. For an ideal  $D_{4h}$  symmetry,  $\delta = 0$ , whereas for the acid molecule<sup>18</sup> with  $C_{2v}$  symmetry and substantial conjugation,  $\delta = 0.221$  Å. In the uncoordinated squarate anions present in compound **1**,  $\delta = 0.056$  Å, very close to the observed value in  $K_2C_4O_4$ <sup>19</sup> ( $\delta = 0.054$  Å), thus indicating a low asymmetry in the  $C_4O_4$  groups.

Hydrogen bonding (involving all the nitrogen and oxygen atoms of the compound) appears to be important in the stabilization of the crystal lattice and leads to the three-dimensional network shown in Figure 2. The main features of the hydrogen bonds are given in Table 3. A part of them

involves the squarate oxygens (O(3) and O(4)), the water molecules (O(5) and O(6)), and the O(21), O(22), and N(21) atoms from the HBIP molecule. The whole of these hydrogen bonds gives pairs of polymeric chains connected through the squarate anions centered on the origins. The rest of the hydrogen bonds connect BIP anions and HBIP molecules.

**Crystal Structure of 2.** Complex **2** is the first example of a characterized copper(II)–BIP complex in which four metal cations are bridged by the squarato ligand in a  $\mu$ -1,2,3,4 coordination mode. The structure is made of infinite chains built from cationic tetranuclear  $\{[Cu(BIP)(OH_2)]_4(\mu-C_4O_4)\}^{2+}$  complex units, two uncoordinated perchlorate anions, and four water molecules of crystallization. The squarato group bridges the copper(II) ions, while BIP acts as a tridentate ligand, connecting through its carboxylate group the tetrameric units along the *a* axis. In the tetranuclear units the Cu(1)–Cu(2), Cu(1)–Cu(2)<sup>iii</sup>, Cu(1)–Cu(1)<sup>iii</sup>, and Cu(2)–Cu(2)<sup>iii</sup> distances are 5.839(2), 5.932(2), 8.281(2), and 8.366(2) Å, respectively. The copper–copper separation between Cu(II) ions belonging to two different molecules along the chains is 8.010(1) Å. Figure 3 shows perspective views of the tetrameric units and the chain structure of the complex. Interatomic bond distances and angles are given in Table 2.

The two crystallographically independent copper(II) ions are pentacoordinated within a distorted square-based pyramid. The basal coordination positions are occupied by two nitrogen atoms of the BIP ligand, a carboxylate oxygen atom of neighboring BIP, and aqueous oxygen atom. The axial position is occupied by a squarato oxygen atom. The Cu–N and Cu–O distances in the basal plane for Cu(1) and Cu(2) range from 1.965(3) to 2.024(3) Å, which are in agreement with previously reported values for several compounds in the Cu–HBIP system.<sup>6,7</sup> On the other hand, the longer Cu–O(squarato) distances (Cu(1)–O(3) = 2.318(3) Å and Cu(2)–O(4) = 2.326(3) Å) are very close to those reported for other copper(II) complexes involving O(squarato) atoms in apical positions.<sup>20</sup> The angles around copper atoms in the basal planes vary from 87.8(1)° to 91.7(1)°. The Cu(1) and Cu(2) atoms are displaced 0.183(1) and 0.110(1) Å, respectively, from the best least-squares plane through the equatorial atoms toward the apical oxygen. Using the  $\tau$  parameter to quantify the distortion of the coordination polyhedra, values of  $\tau = 0.02$  and  $\tau = 0.22$  are obtained for Cu(1) and Cu(2) respectively, thus indicating the predominance of the SP geometry over the TBP one, particularly for the Cu(1) atom.

The bond distances and angles within the BIP ligand have normal values and are in good agreement with the values reported for other BIP derivatives<sup>5–7</sup> as well as that observed in compound **1**. The dihedral angles between the two planar imidazole rings are 22.7(2)° and 22.9(2)° for the BIP molecules coordinated to Cu(1) and Cu(2), respectively. As has been observed in compound **1**, the C–O bond distances satisfy the trend  $C-O_{\text{coord}} > C-O_{\text{uncoord}}$ . The dihedral angles between the COO groups and the imidazole rings are 75.2(3)° and 84.9(2)° for Cu(1) and 71.6(3)° and 84.4(3)° for Cu(2).

(17) Xanthopoulos, C. E.; Sigalas, M. P.; Katsoulos, G. A.; Tsipis, C. A.; Hadjikostas, C. C.; Terzis, A.; Mentzafos, M. *Inorg. Chem.* **1993**, *32*, 3743.

(18) (a) Semmingsen, D. *Acta Chem. Scand.* **1973**, *27*, 3961. (b) Semmingsen, D.; Hollander, F. J.; Koetzle, F. T. *J. Chem. Phys.* **1977**, *66*, 4405.

(19) Macintyre, W. M.; Werkema, M. S. *J. Chem. Phys.* **1964**, *42*, 3563.

(20) (a) Bernardinelli, G.; Deguenon, D.; Soules, R.; Castan, P. *Can. J. Chem.* **1989**, *67*, 1158. (b) Castro, I.; Faus, J.; Julve, M.; Verdager, M.; Monge, A.; Gutierrez-Puebla, E. *Inorg. Chim. Acta* **1990**, *170*, 251. (c) Hosein, H. A.; Jaggernauth, H.; Alleyne, B. D.; Hall, L. A.; Witte, A. J. P.; Williams, D. J. *Inorg. Chem.* **1999**, *38*, 3716.

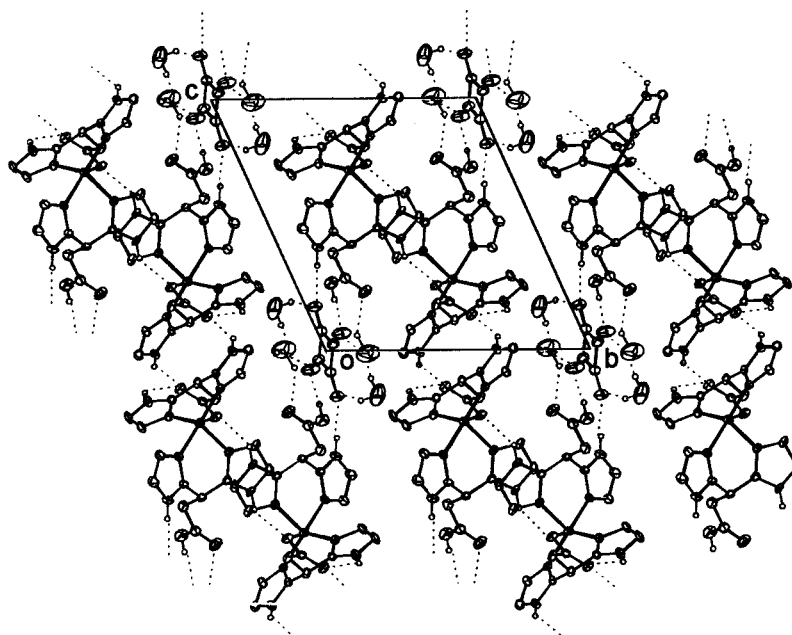


**Figure 2.** Crystal packing of compound **1** as projected on the *bc* planes. Hydrogens of carbon atoms have been omitted.

**Table 3.** Hydrogen Bonds in the Crystal Structures<sup>a</sup>

X—H···Y, Å	X—H, Å	X···Y, Å	H···Y, Å	∠X—H···Y, deg
<b>Complex 1</b>				
O(22)—H(22)···O(4)	0.82	2.535(5)	1.72	178
N(11)—H(11)···O(12) <sup>i</sup>	0.86	2.824(6)	2.09	143
N(14)—H(14)···O(12)	0.86	2.876(5)	2.31	123
N(21)—H(21)···O(3) <sup>ii</sup>	0.86	2.788(6)	1.95	164
N(24)—H(24)···O(11) <sup>iii</sup>	0.86	2.759(5)	2.07	137
O(5)—H(5A)···O(3)	1.01	2.802(5)	1.87	153
O(5)—H(5B)···O(6)	1.01	2.668(6)	1.69	164
O(6)—H(6A)···O(4)	1.06	2.998(5)	2.36	117
O(6)—H(6B)···O(21)	1.00	2.921(6)	2.09	139
<b>Complex 2</b>				
O(13)—H(13B)···O(4) <sup>i</sup>	0.97	2.581(4)	1.62	170
O(23)—H(23A)···O(9)	0.93	2.766(5)	1.84	173
O(23)—H(23B)···O(3)	0.84	2.771(4)	1.93	175
O(9)—H(9A)···O(11)	0.91	2.890(5)	2.01	160
O(9)—H(9B)···O(10)	0.92	2.842(6)	1.99	153
O(10)—H(10A)···O(21) <sup>i</sup>	0.99	2.779(5)	1.80	169
O(10)—H(10B)···O(3)	1.15	3.082(6)	2.16	135
N(11)—H(11)···O(6)	0.86	3.012(6)	2.37	132
N(14)—H(14)···O(12) <sup>ii</sup>	0.86	3.072(5)	2.36	140
N(21)—H(21)···O(22) <sup>iii</sup>	0.86	2.864(5)	2.08	151
N(24)—H(24)···O(7) <sup>iv</sup>	0.86	2.924(6)	2.12	156

<sup>a</sup> Symmetry codes for each complex are as follows: for **1**, (i)  $-x + 1, -y + 1, -z + 2$ ; (ii)  $-x + 1, -y, -z$ ; (iii)  $-x + 1, -y + 1, -z + 1$ ; for **2**, (i)  $-x, -y, -z$ ; (ii)  $-x - 1, -y, -z - 1$ ; (iii)  $-x + 1, -y - 1, -z$ ; (iv)  $x + 1, y - 1, z + 1$ .

The squarate bridge is planar. The dihedral angles between the squarate plane and Cu(1) and Cu(2) equatorial mean planes are  $69.7(1)^\circ$  and  $74.5(1)^\circ$ , respectively. As for compound **1** previously described, the topological parameters for **2** are similar to those expected for a  $C_4O_4$  group with a roughly  $D_{4h}$  symmetry. The value of the  $\delta$  parameter ( $0.032 \text{ \AA}$ ) is close to that obtained for an ionic squarate group (see above), thus indicating a high symmetry within the  $C_4O_4$  group, even greater than that observed in compound **1**, as well as than those reported for the compounds  $[\text{Cu}_4(\text{tren})_4(\text{C}_4\text{O}_4)](\text{ClO}_4)_6$ <sup>21</sup> ( $\delta = 0.042 \text{ \AA}$ ) and  $[\text{Cu}(\text{C}_4\text{O}_4)(\text{H}_2\text{O})_2] \cdot 0.25 \text{ H}_2\text{O}$ <sup>20c</sup> ( $\delta = 0.069 \text{ \AA}$ ) where the squarate ligand also exhibits a  $\mu$ -1,2,3,4-coordination mode.

The crystal packing shown in Figure 4 is mainly determined by the hydrogen bonds listed in Table 3. The tetrameric complex

units are centered around the crystal lattice origins, with the polymeric chains running along the *a* direction. The squarate oxygens (O(3) and O(4)), the copper-coordinated and crystallization water molecules (O(13), O(23), O(9), and O(10)), and the copper-coordinated carboxylate oxygens (O(11) and O(21)), all belonging to the same tetrameric complex unit, are involved in hydrogen bonds within the polymeric chains. The interactions between neighboring polymeric chains are owed to the imidazolyl N—H groups that are acting as hydrogen donors toward the carboxylate oxygens (O(12) and O(22)) and the perchlorate oxygens O(6) and O(7).

**IR and Electronic Spectra.** The IR spectra of **1** and **2** show strong and broad bands in the  $3620\text{--}3200 \text{ cm}^{-1}$  region assignable to  $\nu(\text{OH})$  stretching vibrations of lattice and/or coordinated water molecules with extensive hydrogen bonding.<sup>22</sup> It should be pointed out that complex **2** shows the band at  $3588 \text{ cm}^{-1}$  associated with the presence of a coordinated water. The N—H stretching vibrations of both compounds appear in the  $3200\text{--}3080 \text{ cm}^{-1}$  region, and their frequencies are consistent with the existence of hydrogen bonds between imidazole N—H and several H-acceptor groups.<sup>6</sup> Compound **1** exhibits one  $\nu_{\text{as}}(\text{COO})$  band at  $1710 \text{ cm}^{-1}$  assigned to un-ionized COOH groups, while this band is missing in the spectrum of compound **2**, indicating the loss of the carboxylic proton. On the other hand, both complexes show a single and very strong peak at  $1405 \text{ cm}^{-1}$  assigned to  $\nu_{\text{s}}(\text{COO})$ , this frequency being consistent with a monodentate coordination of the carboxylate group in the complexes.<sup>7,23</sup> Complexes in which the squarate is coordinated through all four oxygen atoms as well as those containing the squarate ion in approximately  $D_{4h}$  symmetry exhibit a strong broad band centered near  $1500 \text{ cm}^{-1}$  assigned to a mixture of C—O and C—C stretching modes.<sup>24</sup> The infrared spectra of both complexes contain a strong band at ca.  $1500 \text{ cm}^{-1}$ , in agreement with the existence of  $C_4O_4$  groups with roughly  $D_{4h}$  symmetry

- (21) Castro, I.; Sletten, J.; Calatayud, M. L.; Julve, M.; Cano, J.; Lloret, F.; Caneschi, A. *Inorg. Chem.* **1995**, *34*, 4903 and references therein.  
 (22) Nakamoto, K. *Infrared and Raman Spectra of Inorganic and Coordination Compounds*, 4th ed.; Wiley: New York, 1986.  
 (23) (a) Battaglia, L. P.; Corradi, A. B.; Menabue, L.; Pellacani, G. C.; Prampolini, P.; Saladini, M. *J. Chem. Soc., Dalton Trans.* **1982**, 781. (b) Abuhijleh, A. L.; Woods, C. *Inorg. Chim. Acta.* **1992**, *194*, 9.

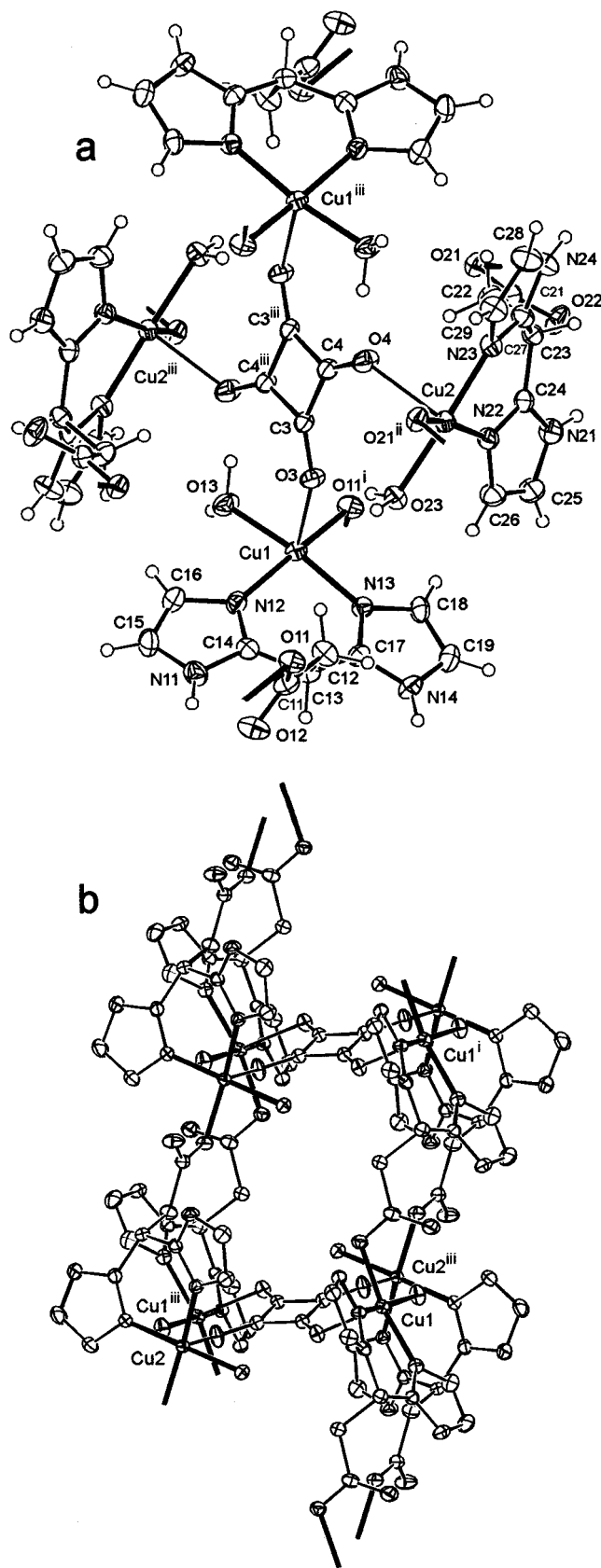


**Figure 3.** ORTEP drawings of compound **2** showing (a) the tetrameric unit with the atom-labeling scheme and (b) the polymeric chains in the crystal structure. Thermal ellipsoids are drawn at the 50% probability level. For symmetry codes see Table 2.

(see structural descriptions). Moreover, the lack of a band at ca. 1800  $\text{cm}^{-1}$  in both complexes is consistent with the absence

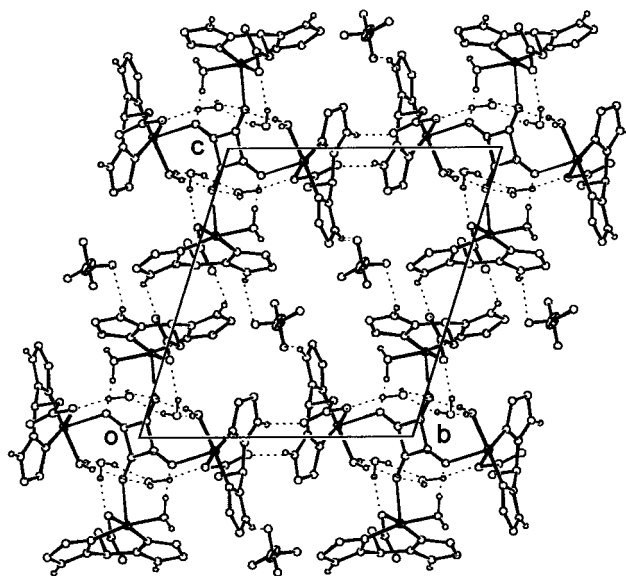


**Figure 4.** Crystal packing of compound **2** as projected on the *bc* planes. Hydrogens of carbon atoms have been omitted.

of localized C=O bonds in the squarate groups. Finally, the IR spectrum of compound **2** shows two bands at 1105 and 620  $\text{cm}^{-1}$  which supports a  $T_d$  symmetry for  $\text{ClO}_4^-$  groups.<sup>25</sup>

The diffuse reflectance spectra of compounds **1** and **2** exhibit very broad absorptions in the visible region with maxima centered at 13500 and 15400  $\text{cm}^{-1}$ , respectively. The position of this absorption for **1** (13500  $\text{cm}^{-1}$ ) is consistent with a five-coordinated copper(II) chromophore with a geometry intermediate between ideal square pyramid and trigonal bipyramid, while the data for **2** (15400  $\text{cm}^{-1}$ ) support an almost regular SP geometry.<sup>26</sup> All these conclusions are in agreement with the results obtained in the X-ray study. Besides this, the electronic spectra of both compounds contain two bands at ca. 31000 and 36400  $\text{cm}^{-1}$  which can be assigned to  $\pi(\text{imidazole}) \rightarrow \text{Cu}(\text{II})$  LMCT and internal  $\pi \rightarrow \pi^*$  squarate transitions.<sup>24d,27</sup>

**Electron Paramagnetic Resonance Spectra.** The Q-band room temperature EPR spectrum of polycrystalline samples of compound **1** (Figure 5) shows an orthorhombic signal with  $g_1 = 2.260$ ,  $g_2 = 2.131$ , and  $g_3 = 2.021$  ( $g_{\text{av}} = 2.137$ ) which remains practically constant from room temperature to 4 K. A coordinate system with *x* and *z* axes close to the quasi-orthogonal Cu–N(23) and Cu–N(22) directions (N(22)–Cu–N(23) angle of 88.9(2)°) can be set up for the  $\text{CuN}_4\text{O}$  chromophore, with a symmetry close to  $C_2$ . Following the vibrational model proposed by Reinen<sup>28</sup> the ground-state wave function of a five-coordinated copper(II) complex can be expressed as follows:

$$\varphi_g = (1 + c^2)^{-1/2} [d_{z^2} + cd_{x^2-y^2}]$$

The mixing coefficient *c* is zero for the trigonal bipyramid ( $d_{z^2}$  ground state) and  $1/\sqrt{3}$  for the square pyramid ( $d_{z^2-y^2}$  ground

- (24) (a) West, R.; Niu, H. Y. *J. Am. Chem. Soc.* **1963**, 85, 2589. (b) Ito, M.; West, R. *J. Am. Chem. Soc.* **1963**, 85, 2580. (c) Baglin, F. G.; Rose, C. B. *Spectrochim. Acta* **1970**, 26A, 2293. (d) Reinprecht, J. T.; Miller, J. G.; Vogel, G. C.; Haddad, M. S.; Hendrickson, D. N. *Inorg. Chem.* **1980**, 19, 927.
- (25) Smékal, Z.; Thronton, P.; Sindelár, Z.; Klicka, R. *Polyhedron* **1998**, 17, 1631.
- (26) (a) Hathaway, B. *J. Coord. Chem. Rev.* **1983**, 52, 87. (b) Lever, A. B. P. *Inorganic Electronic Spectroscopy*, 2nd ed.; Elsevier: Amsterdam, 1986.
- (27) Benarducci, E.; Bharadwaj, P. K.; Krogh-Jespersen, K.; Potenza, J. A.; Schugar, H. J. *J. Am. Chem. Soc.* **1983**, 105, 3860.
- (28) Reinen, D.; Atanasov, M. *Chem. Phys.* **1989**, 136, 27.

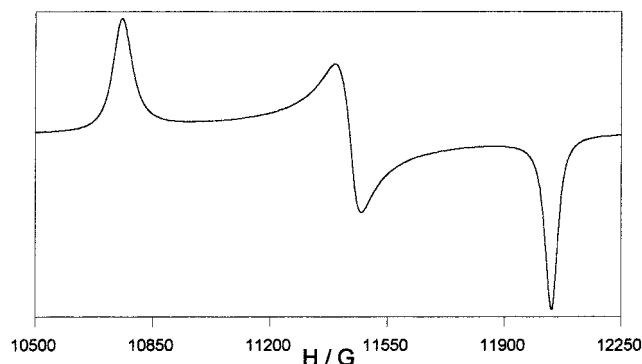


**Figure 5.** EPR powder spectrum (Q-band) of compound **1** at room temperature.

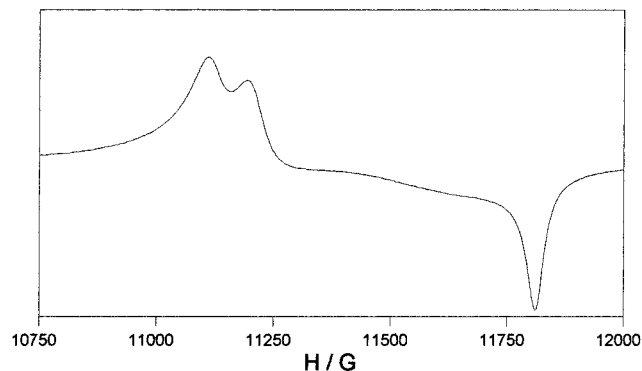


**Figure 6.** EPR powder spectrum (Q-band) of compound **2** at room temperature.

state). The corresponding expressions for the  $g$  values are

$$g_z = g_0 + 8[c^2/(1 + c^2)]u_z$$

$$g_y = g_0 + 2[c^2/(1 + c^2)][1 - \sqrt{3}/c]u_y$$

$$g_x = g_0 + 2[c^2/(1 + c^2)][1 + \sqrt{3}/c]u_x$$

where  $u_i$  are the orbital contributions. Taking  $u_i$  as 0.034 ( $g_{av} = g_0 + 4u_i$ ), the experimental  $g$  values can be nicely reproduced with  $c$  value of  $0.29 \pm 0.03$ , thus implying a ground state for the Cu(II) ions between  $d_{z^2}$  (TBP) and  $d_{x^2-y^2}$  (SP), in excellent agreement with the topology of the copper(II) coordination polyhedron, which is intermediate between both ideal geometries (see above), as shown by the X-ray studies.

In the room temperature powder EPR spectrum (Q-band) of compound **2**, three signals are observed (Figure 6), with the following  $g$  values:  $g_1 = 2.19$ ,  $g_2 = 2.17$ , and  $g_3 = 2.06$  ( $g_{av} = 2.14$ ). The features of this apparently orthorhombic spectrum are not consistent with the observed geometry for the  $\text{CuN}_2\text{O}_2\text{O}'$  chromophores. In particular,  $g_1 = 2.19$  is a very low value for Cu–O bonds and  $g_2 = 2.17$  is evidently too high to be considered as originated by the low orthorhombicity on the Cu–N(O) bonds in the equatorial plane.<sup>29a,b</sup> These facts suggest that the powder spectrum does not reflect the molecular  $g$  values. From the four copper atoms in the unit cell, only two of them, Cu(1) and Cu(2), are magnetically nonequivalent. Then, it may be suggested that the exchange interactions between differently oriented copper chromophores induce a coupled  $\mathbf{g}$  tensor. If the

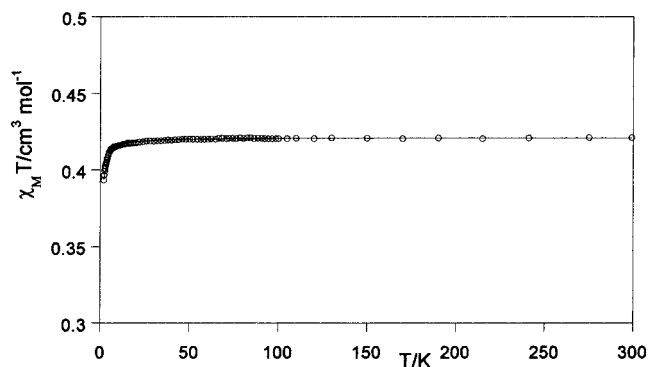


**Figure 7.** Thermal variation of  $\chi_M T$  product for compound **1**.

canting angle is  $2\gamma$ , the following set of values is expected:<sup>30</sup>

$$g_1^{\text{ex}} = (\cos^2 \gamma)g_{\parallel} + (\sin^2 \gamma)g_{\perp}$$

$$g_2^{\text{ex}} = (\cos^2 \gamma)g_{\perp} + (\sin^2 \gamma)g_{\parallel}$$

$$g_3^{\text{ex}} = g_{\perp}$$

The canting angle  $2\gamma$  can be calculated from  $\cos(2\gamma) = (g_1 - g_2)/(g_1 + g_2 - 2g_3)$ . Our experimental  $g$  values yield  $2\gamma = 84^\circ$ , in good agreement with the crystallographic canting angle of  $87^\circ$ , calculated as the angle between the perpendiculars to the mean equatorial planes of the nonequivalent copper sites. Finally, the resultant molecular  $g$  values will be  $g_{\parallel} = 2.305$  and  $g_{\perp} = 2.062$ , which are completely compatible with the roughly square-pyramidal  $\text{CuN}_2\text{O}_2\text{O}'$  chromophores with a  $d_{x^2-y^2}$  ground state.

**Magnetic Properties.** The magnetic susceptibility of compound **1** exhibits a Curie–Weiss dependence. Accordingly, the susceptibility data were fitted to the expression  $\chi_M = C/(T - \theta)$ , affording  $C = 0.421 \text{ cm}^3 \text{ mol}^{-1} \text{ K}$  and  $\theta = -0.13 \text{ K}$ . From the Curie constant  $C = N\beta^2 g^2 S(S + 1)/3k$  with  $S = 1/2$ , a  $g$  value of 2.12 can be obtained, in excellent agreement with that obtained from the EPR spectrum. A plot of  $\chi_M T$  vs the temperature (Figure 7) exhibits a slight decrease at  $T < 10 \text{ K}$ , corresponding to a variation of  $\mu_{\text{eff}}$  between  $1.82 \mu_B$  (at 10 K) and  $1.77 \mu_B$  (at 1.8 K) per copper atom. This decrease is indicative of very weak antiferromagnetic interactions between the copper(II) ions. Taking into account the structure of compound **1**, the magnetic data has been analyzed in terms of a regular  $S = 1/2$  Heisenberg chain using the expression of Brown et al.<sup>31</sup> derived from the numerical results of Bonner and Fisher,<sup>32</sup>

$$\chi_M = \frac{N\beta^2 g^2}{kT} \frac{0.25 + 0.14995x + 0.30094x^2}{1 + 1.9862x + 0.68854x^2 + 6.0626x^3}$$

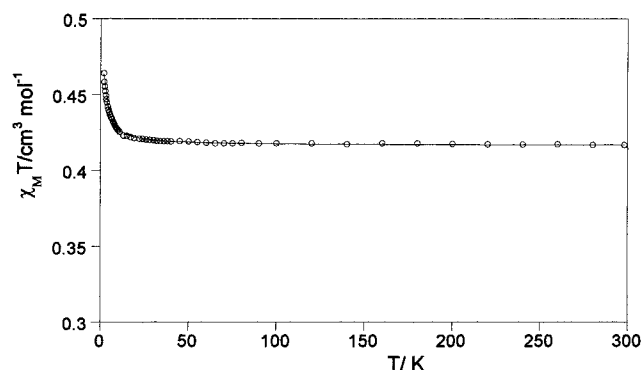
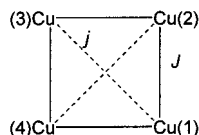
where  $x = |J|/kT$ . The best fit is obtained with  $J = -0.07(1)$  and  $g = 2.12$ , with an agreement factor of  $R = 2.3 \times 10^{-5}$  ( $R$  is defined as  $\sum[(\chi_M)_{\text{obsd}} - (\chi_M)_{\text{calcd}}]^2 / \sum[(\chi_M)_{\text{obsd}}]^2$ ). Such a very low value of the exchange coupling parameter  $J$  may be explained by the topology of the framework bridges. The pathway distance between two nearest-neighboring  $S = 1/2$  spins is about 11.2 Å. According to the limit function proposed by Coffman and Buettner<sup>33</sup> for long-range exchange interactions,

- (29) (a) Reinen, D.; Friebel, C. *Struct. Bonding* **1979**, 37, 1. (b) Atanasov, M.; Zotov, N.; Friebel, C.; Pretov, K.; Reinen, D. *J. Solid State Chem.* **1994**, 108, 37.  
 (30) Henke, W.; Kremer, S.; Reinen, D. *Inorg. Chem.* **1983**, 22, 2858.  
 (31) Brown, D. B.; Donner, J. A.; Hall, J. W.; Eilson, S. R.; Wilson, R. B.; Hodgson, D. J.; Hatfield, W. E. *Inorg. Chem.* **1979**, 18, 2635.  
 (32) Bonner, J. C.; Fischer, M. E. *Phys. Rev. A* **1964**, 135, 640.  
 (33) Coffman, R. E.; Buettner, G. R. *J. Chem. Phys.* **1979**, 83, 2387.

**Table 4.** Relevant Structural and Magnetic Data for Five-Coordinated Copper(II) Systems Containing  $\mu$ -Squarato Bridges

compound <sup>a</sup>	squarato bridging mode	squarato coord site	chromophore	geom	$\tau$ (%)	$\delta^b/\text{\AA}$	$d(\text{Cu}-\text{Cu})/\text{\AA}$	$J/\text{cm}^{-1}$	ref
[Cu <sub>2</sub> (SalNEt <sub>2</sub> )(H <sub>2</sub> O)(C <sub>4</sub> O <sub>4</sub> )]·H <sub>2</sub> O	$\mu$ -1,2	equatorial	CuN <sub>2</sub> O <sub>3</sub>	SP	12	0.140	5.21	-10.3	17
[Cu <sub>2</sub> (phen) <sub>2</sub> (C <sub>4</sub> O <sub>4</sub> )](CF <sub>3</sub> SO <sub>3</sub> ) <sub>2</sub> ·3H <sub>2</sub> O	$\mu$ -1,2	equatorial	CuN <sub>4</sub> O	SP	28	0.237	4.91	-26.4	38
[Cu <sub>2</sub> (bipy) <sub>2</sub> (H <sub>2</sub> O) <sub>4</sub> (C <sub>4</sub> O <sub>4</sub> )](C <sub>4</sub> O <sub>4</sub> H) <sub>2</sub> ·4H <sub>2</sub> O	$\mu$ -1,3	equatorial	CuN <sub>2</sub> O <sub>3</sub>	SP	4	0.020	7.47	~0	20a
[Cu <sub>2</sub> (bipy) <sub>2</sub> (H <sub>2</sub> O) <sub>4</sub> Br <sub>2</sub> (C <sub>4</sub> O <sub>4</sub> )]	$\mu$ -1,3	equatorial	CuBrN <sub>2</sub> O <sub>2</sub>	SP	23	0.060	7.65	~0 <sup>c</sup>	20a
[Cu <sub>2</sub> (bipy) <sub>2</sub> (H <sub>2</sub> O) <sub>4</sub> (C <sub>4</sub> O <sub>4</sub> )](NO <sub>3</sub> ) <sub>2</sub>	$\mu$ -1,3	equatorial	CuN <sub>2</sub> O <sub>3</sub>	SP	14	0.020	7.69	~0	36
[Cu <sub>2</sub> (terpy) <sub>2</sub> (H <sub>2</sub> O) <sub>2</sub> (C <sub>4</sub> O <sub>4</sub> )](ClO <sub>4</sub> ) <sub>2</sub>	$\mu$ -1,3	equatorial	CuN <sub>3</sub> O <sub>2</sub>	SP	8	0.061	7.47	-3.6	36
[Cu <sub>2</sub> (mpym)(H <sub>2</sub> O)(C <sub>4</sub> O <sub>4</sub> )]·2H <sub>2</sub> O	$\mu$ -1,3	equatorial	CuN <sub>2</sub> O <sub>3</sub>	TBP	70	0.081	7.86	~0	37
[Cu <sub>2</sub> (bipy) <sub>2</sub> (C <sub>4</sub> O <sub>4</sub> )](CF <sub>3</sub> SO <sub>3</sub> ) <sub>2</sub> ·6H <sub>2</sub> O	$\mu$ -1,3	equatorial	CuN <sub>4</sub> O	SP	15	0.058	7.31	-8.6	38
[Cu <sub>4</sub> (tren) <sub>2</sub> (C <sub>4</sub> O <sub>4</sub> )](ClO <sub>4</sub> ) <sub>6</sub>	$\mu$ -1,2,3,4	axial	CuN <sub>4</sub> O	TBP	86/93	0.040	5.29/7.46 <sup>d</sup>	-19.0/-0.8 <sup>e</sup>	21
[Cu <sub>4</sub> (BIP) <sub>4</sub> (H <sub>2</sub> O) <sub>4</sub> (C <sub>4</sub> O <sub>4</sub> )](ClO <sub>4</sub> ) <sub>2</sub>	$\mu$ -1,2,3,4	axial	CuN <sub>2</sub> O <sub>3</sub>	SP	22/2	0.032	5.89/8.32 <sup>d</sup>	~0/+0.8 <sup>e</sup>	this work

<sup>a</sup> SalNEt<sub>2</sub> = *N*-(2-(diethylamino)ethyl)-salicylideneamine, phen = 1,10-phenanthroline, bipy = 2,2'-bipyridine, terpy = 2,2',6',2''-terpyridine, mpym = 4-methoxy-2-(5-methoxy-3-methyl-1*H*-pyrazol-1-yl)-6-methylpyrimidine, tren = tris(2-aminoethyl)amine. <sup>b</sup> See text. <sup>c</sup>  $\theta = +0.86$  K. <sup>d</sup> Mean values for adjacent and nonadjacent copper atoms, respectively. <sup>e</sup> Corresponding to  $\mu$ -1,2 and  $\mu$ -1,3 pathway squarato bridge.

**Figure 8.** Thermal variation of  $\chi_M T$  product for compound **2**.**Scheme 2**

which has the form  $-J = (1.35 \times 10^7)\exp(-1.8R)$ , for a copper-copper exchange pathway distance of ca. 11 Å the absolute  $J$  value would be expected to be less than 0.02  $\text{cm}^{-1}$ . In addition, this extended pathway involves two C-C  $\sigma$  bonds, which offer a very poor support for the interactions.<sup>34</sup> Therefore, the effectiveness of the propionate arm pathway to support significant magnetic exchange interactions between the copper atoms may be considered as negligible.

The magnetic measurements of compound **2** (Figure 8) shows a Curie-Weiss behavior in the range 10–300 K, with a Weiss temperature of  $\theta = +0.12$  K and a Curie constant  $C = 0.417$   $\text{cm}^3 \text{K mol}^{-1}$  (like that expected for uncoupled copper(II) ions). At temperatures below 10 K  $\chi_M T$  product exhibits an increase corresponding to a variation of  $\mu_{\text{eff}}$  from 1.84  $\mu_B$  (at 10 K) to 1.93  $\mu_B$  (at 2.0 K). This magnetic behavior indicates the existence of weak ferromagnetic interactions between the copper(II) ions. To date, only one  $\mu$ -squarato bridged copper(II) system showing ferromagnetic behavior has been reported.<sup>20a</sup> As we have discussed above, the effectiveness of the propionate-bridge pathway to support significant magnetic interactions between the copper atoms may be considered as negligible. Taking into account this consideration, and the crystal structure, compound **2** might be considered, from a magnetic point of view, as an assembly of quasi-isolated  $[\{\text{Cu}(\text{BIP})(\text{OH}_2)\}_4(\mu$ -

C<sub>4</sub>O<sub>4</sub>)] tetramers. Assuming that the four copper ions are equivalent (Scheme 2), then the spin system involves two exchange-coupling constants,  $J$  and  $j$ . Therefore, the susceptibility data can be fitted to a theoretical expression for the magnetic susceptibility derived from the following Hamiltonian.<sup>21,35</sup>

$$\hat{H} = -J(\hat{S}_1 \cdot \hat{S}_2 + \hat{S}_1 \cdot \hat{S}_4 + \hat{S}_2 \cdot \hat{S}_3 + \hat{S}_3 \cdot \hat{S}_4) - j(\hat{S}_1 \cdot \hat{S}_3 + \hat{S}_2 \cdot \hat{S}_4)$$

where  $J = J_{12} = J_{14} = J_{23} = J_{34}$  and  $j = J_{13} = J_{24}$ . The theoretical expression for the magnetic susceptibility is

$$\chi_M = (2N\beta^2 g^2/kT)W/Z \quad (1)$$

where

$$W = \exp[(2j - J)/kT] + 2 \exp(j/kT) + 5 \exp[(J + 2j)/kT] \quad (2)$$

and

$$Z = 1 + \exp[(2j - 2J)/KT] + 3 \exp[(2j - J)/KT] + 5 \exp[(J + 2j)/KT] + 6 \exp(j/kT) \quad (3)$$

Magnetic data were least-squares-fitted to eq 1 (solid line in Figure 8), with the  $g$  value fixed at 2.14 (obtained from the EPR spectrum), to yield exchange-coupling constants of  $J = -0.01(1)$   $\text{cm}^{-1}$  and  $j = +0.81(1)$   $\text{cm}^{-1}$ , with an agreement factor  $R = 2.8 \times 10^{-4}$ .

The lack of significant antiferromagnetic coupling between the copper(II) ions may be understood on the basis of the structural features of the bridging network together with the nature of the orbitals involved in the exchange interaction. As is well-known, the squarato group provides a poor support for the exchange interaction, related to the stabilization of the ligand orbitals by  $\pi$ -delocalization in the C<sub>4</sub>O<sub>4</sub> ring.<sup>35,37</sup> Table 4 shows the most relevant data for the structural and magnetically characterized  $\mu$ -squarato-bridged copper(II) systems (restricted to five-coordinated copper(II) complexes). In general, the greatest values of the exchange coupling parameter are observed in systems with  $\mu$ -1,2-squarato bridges.<sup>38</sup>

(35) Tangoulis, V.; Raptopoulou, C. P.; Paschalidou, S.; Tsohos, A. E.; Bakañbassi, E. G.; Terzis, A.; Perlepes, S. P. *Inorg. Chem.* **1997**, *36*, 5270.

(36) Solans, X.; Aguiló, M.; Gleizes, A.; Faus, J.; Julve, M.; Verdager, M. *Inorg. Chem.* **1990**, *29*, 775.

(37) Benetó, M.; Soto, L.; García-Lozano, J.; Escrivà, E.; Legros, J.-P.; Dahan, F. *J. Chem. Soc., Dalton Trans.* **1991**, 1057.

(38) Castro, I.; Calatayud, M. L.; Sletten, J.; Lloret, F.; Julve, M. *Inorg. Chim. Acta* **1999**, *287*, 173.

(34) Hay, P. J.; Thibeault, J. C.; Hoffmann, R. *J. Am. Chem. Soc.* **1975**, *97*, 4886.



As is well-known, the magnetic constant  $J$  can be expressed as a sum of both ferromagnetic ( $J_F$ ) and antiferromagnetic ( $J_{AF}$ ) contributions. The extent of the antiferromagnetic interactions depends on the overlap of magnetic orbitals. This, in turn, arises basically from the overlap of spin-carrying orbitals on the metals and suitable orbitals on the bridging system. As discussed above, the unpaired electron of the copper(II) ions in **2** is essentially described by magnetic orbitals built from the  $d_{x^2-y^2}$  metallic orbitals—with a small contribution from  $d_z^2$  orbitals—localized in a plane roughly perpendicular to the bridging edge for the copper atoms. Such orientation does not favor a significant overlap. This fact, besides the poor support of exchange provided by the  $\mu$ -squarato bridges groups—which exhibit a low asym-

metry and consequently extended  $\pi$ -delocalization within the  $C_4O_4$  ring—precludes the existence of significant antiferromagnetic interaction. These considerations taken together explain the  $J_{AF} \sim 0$  and the weak ferromagnetic interaction observed.

**Acknowledgment.** We are grateful to the DGICYT (PB98-1453) for financial support. We thank Drs. F. Lloret and L. Lezama for their assistance with susceptibility and EPR measurements, respectively.

**Supporting Information Available:** Crystallographic information in CIF format. This material is available free of charge via the Internet at <http://pubs.acs.org>.

IC0106571